PROCEEDINGS OF SCIENCE

Final COMPASS results on the spin-dependent structure functions g_1^p and g_1^d in the deep-inelastic and nonperturbative regions

Barbara Badelek[*†]
Faculty of Physics, University of Warsaw
E-mail: badelek@fuw.edu.pl

This paper summarizes the COMPASS Collaboration legacy on measurements of the proton and deuteron spin-dependent structure functions, g_1^p and g_1^d at $Q^2 < 1$ (GeV/c)^2 and $Q^2 > 1$ (GeV/c)^2. In both regions and at the lowest measured x, $g_1^d(x)$ is consistent with zero while $g_1^p(x)$ is positive. This is the first time that the spin effects are observed at such low values of x. The NLO QCD fit of g_1 world data gives well constrained quark helicity distributions; gluons are poorly determined. Quark helicity contribution to nucleon spin is $0.26 < \Delta\Sigma < 0.36$. From the COMPASS data alone the Bjorken sum rule is verified to 9% accuracy and the extracted flavour-singlet axial charge is $a_0(Q^2 = 3\ (\mathrm{GeV}/c)^2) = 0.32 \pm 0.02_{\mathrm{stat.}} \pm 0.04_{\mathrm{syst.}} \pm 0.05_{\mathrm{evol.}}$.

XXV International Workshop on Deep-Inelastic Scattering and Related Subjects
3-7 April 2017
University of Birmingham, UK

[*]Speaker.
[†]On behalf of COMPASS Collaboration.

© Copyright owned by the author(s) under the terms of the Creative Commons Attribution-NonCommercial-NoDerivatives 4.0 International License (CC BY-NC-ND 4.0).

1. Introduction

Spin-dependent aspects of the nucleon structure are still less known than the the spin-averaged ones. In the last two decades several new experiments were set up to study the longitudinal spin structure of the nucleon in even more detail. These experiments included COMPASS at CERN which uses the CERN SPS muon beam line at energies 160 GeV and 200 GeV in particular for the measurements of double spin cross-section asymmetries in the lepton-nucleon scattering.

2. COMPASS spectrometer and method of extraction of A_1 and g_1

The COMPASS spectrometer is an open, two-staged apparatus, with about 350 detector planes, calorimetry, particle identification and a large, solid state polarised target. More details are given in Ref. [1].

The tertiary M2 beam of the CERN SPS delivers a naturally polarised muon beam with a polarisation of about 80%. Momentum and trajectory of each beam particle and of secondary particles are measured. The polarised target, about 1.2m long contained NH_3 or ^{6}LiD materials, polarised to about 90% (protons) and 50% (deuterons) respectively, held in two (before 2006) or three ($\geq$ 2006) cells. The two outer cells (30 cm each) are polarised oppositely to the inner one (60 cm long) allowing a simultaneous measurement for both target polarisations, to partially cancel the systematic uncertainties. The polarisation direction of cells was regularly inversed.

A cross-section asymmetry is extracted from a difference in number of interactions in parallel and antiparallel oriented longitudinal spins of muon and target proton/deuteron. This asymmetry when divided by the deplarisation factor is approximately equal to asymmetry A_1 of cross sections for the absorption of transversely polarised virtual photons by a proton/deuteron. The latter, together with the knowledge of the spin-averaged structure function F_2 and the ratio R, give the spin-dependent structure function g_1. The parameterisation of $F_2^{p,d}$ and R were taken from Refs [2] and [3], respectively.

3. Results on A_1^p and g_1^p at $Q^2 > 1$ (GeV/c)^2

Results presented here, Fig.1, are based on data collected in 2007 [4] and 2011 [5] with the NH_3 target. In 2011 the beam energy was increased to 200 GeV to access higher values of Q^2 and lower values of x. Results on A_1^p and g_1^p for the two energies agree very well with each other and with the world data, Fig.1 thus illustrating their weak dependence on Q^2. A very interesting fact is a positivity of $g_1^p(x)$ down to the lowest measured values of x.

4. Results on A_1^d and g_1^d at $Q^2 > 1$ (GeV/c)^2

Results presented here, Fig.2, are based on data collected in 2002-2004 [11] and 2006 [12] with the ^{6}LiD target. Results on A_1^d and g_1^d from both samples agree very well with each other and with the world data, Fig.2 thus illustrating their weak dependence on Q^2. Contrary to the behaviour of $g_1^p(x)$ and to the hints from SMC [2] the $g_1^d(x)$ is compatible with zero at lowest measured x.

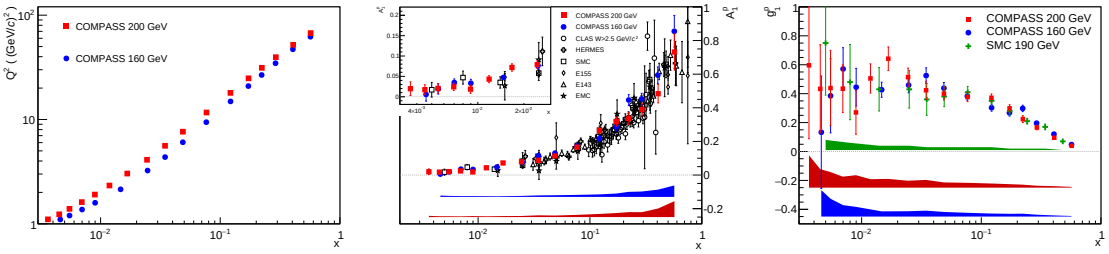

Figure 1: COMPASS results for A_1^p and g_1^p for the muon energies 160 GeV [4] and 200 GeV [5] in the DIS region. **Left:** mean values of Q^2 vs x. **Middle:** A_1^p vs x for both energies and at measured values of Q^2, compared to the other world data (EMC [6], CLAS [7], HERMES[8], E143 [9], E155 [10] and SMC [2]. **Right:** g_1^p vs x for both energies and at measured values of Q^2, compared to the SMC measurements [2]. Bands at the bottom indicate the systematic uncertainties of the COMPASS data at 160 GeV (blue), 200 GeV (red) and SMC at 190 GeV (green).

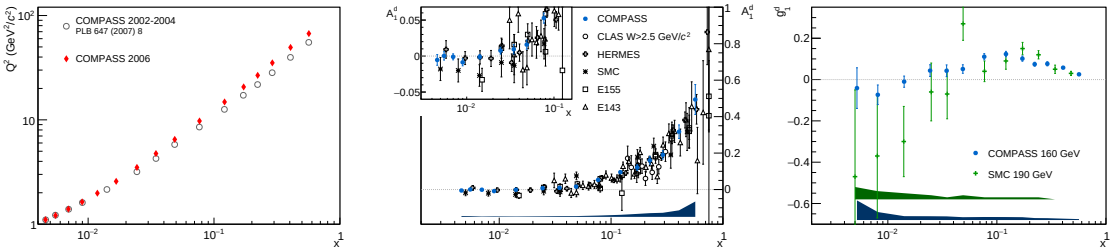

Figure 2: COMPASS results for A_1^d and g_1^d for the data collected in 2002-2004 [11] and 2006 [12] in the DIS region. **Left:** mean values of Q^2 vs x. **Middle:** A_1^d vs x for both samples and at measured values of Q^2, compared to the other world data (CLAS [7], HERMES[8], SMC [2], E155 [13] and E143 [9]. **Right:** g_1^d vs x for both samples combined and at measured values of Q^2 compared to the SMC measurements [2]. Bands at the bottom indicate the systematic uncertainties of the COMPASS data (blue) and SMC (green).

5. NLO QCD analysis of the g_1 world data

The Q^2 dependence for the world data of the proton and deuteron structure functions g_1 is shown in Fig.3. Crucial for the QCD analysis are the high Q^2 data of COMPASS. The g_1 appears to show only weak scaling violation and thus a weak sensitivity to the helicity distribution of gluons.

In the fit all the world inclusive measurements of g_1^p, g_1^d, $g_1^{^3He}$ at $W^2 > 10$ (GeV/c^2)^2 and $Q^2 > 1$ (GeV/c)^2 were used, a total of 495 data points (138 of COMPASS). The $\overline{\text{MS}}$ renormalisation and factorisation schemes were assumed. Fitted was the gluon helicity Δg, the singlet $\Delta q^S = \Delta(u+\bar{u}) + \Delta(d+\bar{d}) + \Delta(s+\bar{s})$ and two nonsinglet distributions $\Delta q_3 = \Delta(u+\bar{u}) - \Delta(d+\bar{d})$ and $\Delta q_8 = \Delta(u+\bar{u}) + 2\Delta(d+\bar{d}) - \Delta(s+\bar{s})$. At $Q_0^2 = 1$ (GeV/c)^2 the x-dependence of the distributions was parameterised as: $\Delta f_k(x) = \eta_k \left[x^{\alpha_k}(1-x)^{\beta_k}(1+\gamma_k x)\right] / \left[\int_0^1 x^{\alpha_k}(1-x)^{\beta_k}(1+\gamma_k x)\mathrm{d}x\right]$ where $k = s, 3, 8, g$ and η_k is the first moment of $\Delta f_k(x)$ at Q_0^2. The nonsinglet moments are fixed by the baryon decay constants: η_3 = F+D, η_8 = 3F-D when the flavour SU(2) and SU(3) symmetries are assumed; for the nonsinglet and gluon distributions, γ=0. For the gluons, β was fixed at the value of unpolarised distribution in the MSTW parameterisation [14]. At each iteration step, the positivity constraint was imposed: $|\Delta q(x)| < q(x)$ and $|\Delta g(x)| < g(x)$ at $Q^2 = 1$ (GeV/c)^2. Only

statistical errors were considered in the fit; normalisations of data sets varied. The number of free parameters was 11. Systematic studies comprised: changing values of Q_0^2, of the unpolarised parton distribution set and of the form of the $Q_0^2 = 1$ (GeV/c)^2 parameterisations. Two kinds of the latter give equally good fit: the one with $\gamma_S = 0$ (implying a negative gluon distribution) and the one where γ_S is a free parameter (positive gluon distribution).

Results of the fit are shown in Figs 3 and 4. In the latter the singlet and the parton helicity distributions are presented. Gluon helicity is poorly constrained, while the contribution from quarks to the nucleon spin (or the first moment of the singlet distrtibution), $\Delta\Sigma$ is: $0.26 < \Delta\Sigma < 0.36$. The largest uncertainty on the determination of $\Delta\Sigma$ comes from the uncertainty on the Δg.

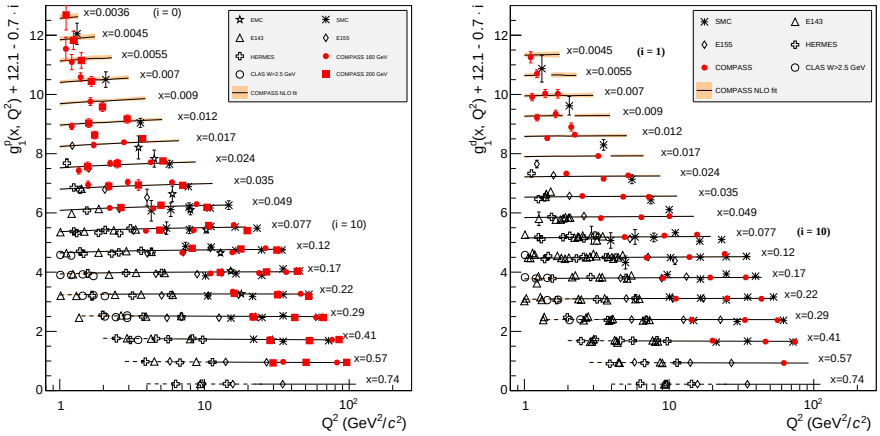

Figure 3: World data on g_1^p (**left**), [5] and g_1^d (**right**), [12] as a function of Q^2 for various values of x. The solid line represents the NLO QCD fit for $W^2 > 10$ (GeV/c)^2, the dashed one – an extension to lower values of W^2.

6. First moments of structure functions g_1 and g_1^{NS}

The first moment Γ_1^d of g_1^d allows for a determination of the flavour-singlet axial charge a_0 with the axial charge a_8 as an additional input. The COMPASS data on g_1^d gave: $a_0(Q^2 = 3$ (GeV/c)^2)$= 0.32 \pm 0.02_{\text{stat.}} \pm 0.04_{\text{syst.}} \pm 0.05_{\text{evol.}}$, [12], consistent with the value of a_0 obtained from the COMPASS NLO QCD fit [5]. In the $\overline{\text{MS}}$ scheme a_0 is identified with the total quark helicity contribution to the nucleon spin, $a_0 \overset{\overline{\text{MS}}}{=} \Delta\Sigma$.

The non-singlet structure function, $g_1^{NS}(x, Q^2)$, defined as: $g_1^{NS} = g_1^p - g_1^n = 2\left[g_1^p - g_1^N\right] = 2\left[g_1^p - g_1^d/(1 - 1.5\omega_D)\right]$ (here ω_D is a contribution of the D-state in the deuteron, $\omega_D = 0.05 \pm 0.02$) is presented in Fig.4 [5]. Its first moment is connected to the fundamental Bjorken sum rule [15]. Extraction of the Γ_1^{NS} from the data led to a validation of the sum rule at the level of 9%, see Ref.[5] for the details.

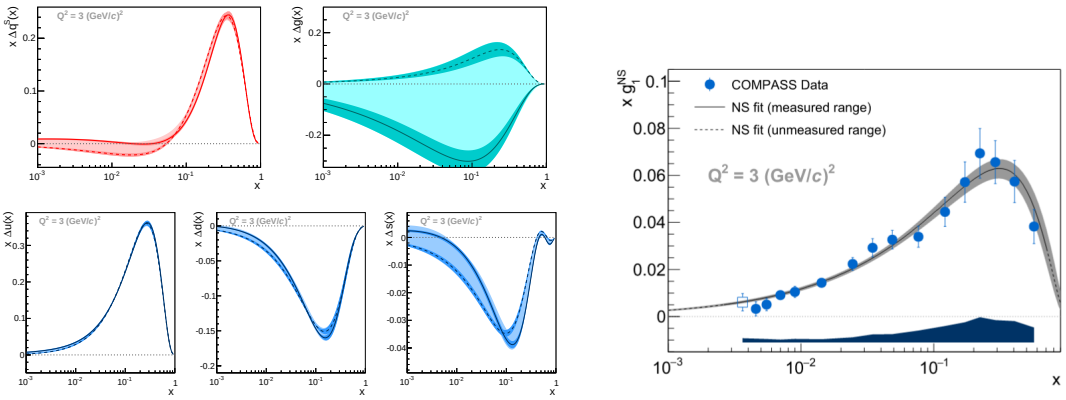

Figure 4: Results of the QCD fits to g_1 world data at $Q^2 = 3$ (GeV/c)^2 for two sets of functional shapes [5], see text. **Left-top:** singlet $x\Delta q^S(x)$ and gluon distribution $x\Delta g(x)$. **Left-bottom:** distributions of $x[\Delta q(x) + \Delta\bar{q}(x)]$ for different flavours (u, d and s). Continuous lines correspond to the fit with $\gamma_S = 0$, long dashed lines to the one with $\gamma_S \neq 0$. The dark bands represent the statistical uncertainties, only. The light bands, which overlay the dark ones, represent the systematic uncertainties. **Right:** Values of $xg_1^{NS}(x)$ at $Q^2 = 3$ (GeV/c)^2 compared to the non-singlet NLO QCD fit using COMPASS data only. The band around the curve represents the statistical uncertainty of the NS fit.

7. Longitudinal double spin asymmetry A_1 and spin-dependent structure function g_1 in the nonperturbative $Q^2 < 1$ (GeV/c)^2 region

Contrary to the studies in the deep inelastic region, the behaviour of g_1^p at lower Q^2 is largely unknown; the g_1^d was however measured earlier, [16]. The low-Q^2-region is governed by 'soft' physics processes and the transition to the region of higher Q^2 is still not understood. For fixed-target experiments, the values of $Q^2 < 1$ (GeV/c)^2 are strongly correlated with low values of x where also physics of large parton densities sets up.

Measurements at low x and low Q^2 are scarce as they put high demands on event triggering and reconstruction. They were performed only by the Spin Muon Collaboration on proton and deuteron [2] and by COMPASS on the deuteron [16]. The latter, very precise results do not reveal any spin effects in g_1^d over the whole measured interval of x. Here we present new results obtained on the A_1^p and g_1^p in the region 0.0062 (GeV/c)$^2 < Q^2 < 1$ (GeV/c)^2 and $4\times10^{-5} < x < 4\times10^{-2}$, $0.1 < y < 0.9$ and for $W > 5$ GeV. Four different 2-dimensional grids of kinematic variables are used: $(x,Q^2),(\nu,Q^2),(x,\nu)$ and (Q^2,x); an example is shown in Fig.5 (see Ref. [17] for the details).

A resulting asymmetry A_1^p and structure function g_1^p are presented in Fig. 5. Very clear spin effects in $g_1^p(x)$ are seen at all x. There exist several models describing $g_1^p(x,Q^2)$, valid at low Q^2 and low x [19, 20, 21, 22]. Predictions of one of them, [20], based on GVMD ideas supplemented by the Regge formalism are shown in Fig.5. The models describe the general trend in the data and point towards substantial perturbative and non-perturbative contributions to g_1^p at *any* Q^2.

8. Conclusion

Results presented in this paper constitute the COMPASS legacy on $g_1^p(x,Q^2)$ and $g_1^d(x,Q^2)$ both for the DIS ($Q^2 >1$ (GeV/c)^2) and nonperturbative ($Q^2 <1$ (GeV/c)^2) regions. At the same

time they are the state-of-the-art measurements that only can be surpassed by measurements with polarised beams of the future Electron Ion Collider.

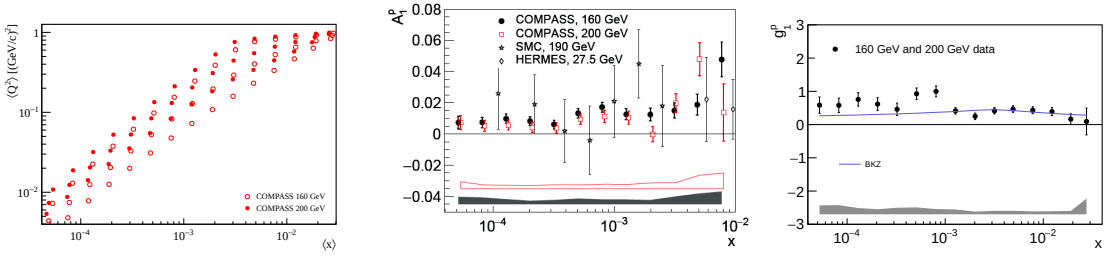

Figure 5: COMPASS results for g_1^p at low Q^2 for two muon energies. **Left:** kinematic range of g_1^p measurements in (Q^2,x) variables. **Middle:** asymmetry A_1^p as a function of x at measured values of Q^2 compared to the data of HERMES [8] and SMC [2, 18]. No Q^2 dependence is observed. **Right:** combined $g_1^p(x)$ data; the curve is from Ref.[20].

References

[1] COMPASS Collaboration, P. Abbon et al., Nucl. Instrum. Meth. A **577** (2007) 455.

[2] SM Collaboration, B. Adeva et al., Phys. Rev. D **58** (1998) 112001.

[3] E143 Collaboration, K. Abe, et al., Phys. Lett. B **452** (1999) 194; see also Appendix in [16].

[4] COMPASS Collaboration, M.G. Alekseev, et al., Phys. Lett. B **690** (2010) 466.

[5] COMPASS Collaboration, C. Adolph et al., Phys. Lett. B **753** (2016) 18.

[6] EM Collaboration, J. Ashman, et al., Phys. Lett. B **206** (1988) 364; Nucl. Phys. B **328** (1989) 1.

[7] CLAS Collaboration, K. V. Dharmawardane, et al., Phys. Lett. B **641** (2006) 11.

[8] HERMES Collaboration, A. Airapetian, et al., Phys. Rev. D **75** (2007) 012007.

[9] E143 Collaboration, K. Abe, et al., Phys. Rev. D **58** (1998) 112003.

[10] E155 Collaboration, P.L. Anthony, et al., Phys. Lett. B **493** (2000) 19.

[11] COMPASS Collaboration, V.Yu. Alexakhin, et al., Phys. Lett. B **647** (2007) 8.

[12] COMPASS Collaboration, C. Adolph, et al., Phys. Lett. B **769** (2017) 34.

[13] E155 Collaboration, P.L. Anthony, et al., Phys. Lett. B **463** (1999) 339.

[14] MSTW, A.D. Martin et al., Eur. Phys. J. C **63** (2009) 189.

[15] J.D. Bjorken, Phys. Rev., **148** (1966) 1467; *ibid.* D **1** (1970) 1376.

[16] COMPASS Collaboration, V. Yu. Alexakhin, et al., Phys. Lett. B **647** (2007) 330.

[17] COMPASS Collaboration, C. Adolph, et al., to be submitted to Phys. Lett. B.

[18] SM Collaboration, B. Adeva et al., Phys. Rev.D **60** (1999) 072004; erratum *ibid.*, D **62** (2000) 079902.

[19] B. Badelek, J. Kwiecinski, J. Kiryluk, Phys. Rev. D **61** (2000) 014009.

[20] B. Badelek, J. Kwiecinski, B. Ziaja, Eur. Phys. J. C **26** (2002) 45 and private communication (2017).

[21] B.I. Ermolaev, M. Greco, S.I. Troyan, Eur. Phys. J. C **50** (2007) 823; *ibid.* C **51** (2007) 859.

[22] W. Zhu, J. Ruan, Int. J. Mod. Phys. E **24** (2015) 1550077.